Decomposition of the Factors That Govern Binding Site Preference in a Multiple Rotaxane

Joseph P. Angelo and Karl Sohlberg*

Department of Chemistry, Drexel University, 3141 Chestnut Street, Philadelphia, Pennsylvania 19104

Received: December 2, 2008; Revised Manuscript Received: May 1, 2009

A particularly interesting class of multiple rotaxanes consists of complexes where one long shaft threads two rings. If the shaft contains three or more potential binding sites for the rings, multiple co-conformations are possible. Such a complex is a molecular topological analogue to an abacus. Here we address the question, how does strength of ring binding to the shaft vary with respect to position on the shaft? Previous studies have found that a shaft with three binding sites exhibits strongest ring binding at the center site. Here a five-binding-site shaft is studied. We employ a novel method to partition the total energy of the system into contributions from intercomponent binding and intracomponent distortion. The method uses the output of quantum mechanical electronic structure calculations to determine fitting parameters in a set of coupled equations. The solution of the equations yields the energy partitioning and reveals the influence of long-range intercomponent interactions.

Introduction

Mechanically interlocked molecules, especially rotaxanes,[1,2] are currently of considerable interest for their potential as nanomachine components. A rotaxane is a molecular complex that contains a long dumbbell-shaped molecule (termed the "shaft") that threads a ring-shaped molecule without actually bonding to it. Since the components cannot be dissociated without breaking at least one chemical bond, they are mechanically linked, but due to the absence of any *inter*component chemical bond, they remain chemically independent. *Multiple rotaxanes* are rotaxanes containing more than two mechanically interlocked molecules. A particularly interesting class of multiple rotaxanes is that consisting of complexes where one long shaft threads two or more rings. The relative positions of the rings along the shaft can be controlled using intermolecular interaction forces.[3−6] For example, if the rings are crown ethers, the electron-rich cavities of the rings will experience electrostatic attraction for protonated amine (ammonium) groups placed along the shaft. This crown-ether/ammonium interaction chemistry is one of the most commonly employed motifs used in the construction of rotaxanes.[7−9] The ammonium moieties effectively serve as binding sites for the rings. If the number of binding sites on the shaft is greater than the number of rings, there are multiple distinct classes of co-conformations. This multiple stability could conceivably form the basis for a molecular abacus. To build the knowledge base that will facilitate the design of such a nanoscale machine, here we address the question of how the strength of ring binding to the shaft varies in energy with respect to position on the shaft.

Multiple rotaxane complexes are rather large (from the perspective of molecular modeling). Previous theoretical research[5] focused on one of the smallest [3]rotaxanes that has been synthesized,[10] i.e., a [3]rotaxane with three binding sites and two rings. It had been inferred from earlier experiments[11] that co-conformations in which one of the rings resides on the center binding site are energetically favored. In the theoretical work it was found that ring−ring interactions are negligible, implying that ring−shaft intercomponent interactions decide the co-conformational preference.[5] Since the ring(s) of a rotaxane is (are) not covalently bonded to the shaft, it is (they are) free to rotate about the shaft and move along it. Previous theoretical studies of rotaxanes that employ crown-ether/ammonium interaction chemistry[5,12] have confirmed, however, that the complex optimizes when the crown-ether ring is located around a positively charged ammonium group. A potential energy curve, produced by moving a ring molecule along a shaft reveals that stability is only found when the ring is in the proximity of a binding site.[6,13] In fact, if a ring is placed between bonding sites, upon optimization it spontaneously moves to an adjacent binding site.[5] This finding allows the search space for stable co-conformations to be narrowed. Instead of testing the ring along the entire length of the shaft, it is sufficient to focus on structures with the rings centered on binding sites.[6] We can capitalize on this finding to study larger multiple rotaxanes. Here, a [3]rotaxane with a five-binding-site shaft is studied.

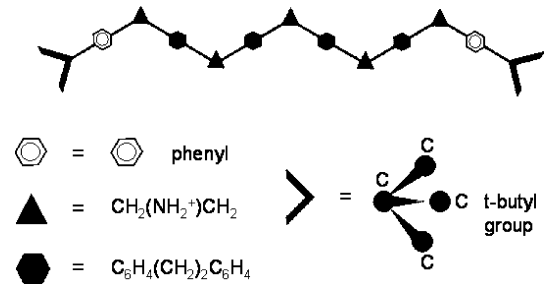

Figure 1. Schematic representation of the five-site shaft.

Methods

We consider a [3]rotaxane in which a long dumbbell-shaped molecule threads *two* crown ether rings. Five protonated amino groups along the shaft attract the electron-rich cavities in the centers of the crown-ether ring molecules and serve therefore as the ring-binding sites. A schematic of the complex is shown in Figure 1. The crown-ether ring is shown in Figure 2. For construction of the full [3]rotaxane, the starting structure for the shaft was taken to be "straight" because structural analysis of the isolated shaft showed the "straight" form to be energetically favored. There are numerous rotatable dihedral angles

10.1021/jp8106099 CCC: $40.75
Published on Web 05/26/2009

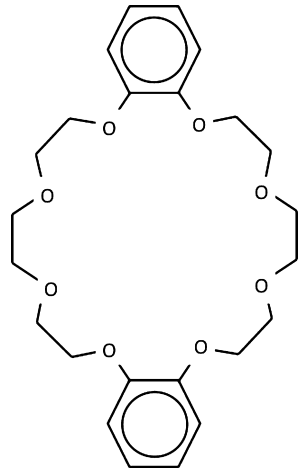

Figure 2. Schematic representation of the dibenzo-24-crown-8 ring used in this study. Its highly electron-rich center prefers to bind to cationic ammonium sites.

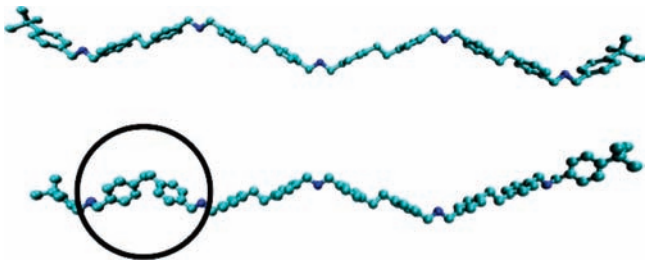

Figure 3. Two stable conformations of the isolated shaft. The shaft with the circled "kink" is ca. 1.3 kcal/mol higher in energy than the "straight" form.

along the shaft. The potential energy curve for rotation about the center-most CCCC dihedral angle exhibits a single minimum at 180°. The same is true for the center-most CCNC dihedral angle. While generally the dihedral angles are lowest in energy in the "anti"-conformation, it is possible to introduce a "kink" along the shaft. One such stable conformation of the isolated shaft is compared to the straight shaft in Figure 3. The introduction of such a kink along the shaft has an energy cost of ca. 1.3 kcal/mol.

Given that the rings of the [3]rotaxane that are considered here can be expected to preferentially locate on or around the ammonium binding sites, there are six possible classes of co-conformations, as shown in Figure 4. For each class of co-conformations, a set of starting structures was generated to take into account the freedom of the ring to rotate about the shaft. The first ring was rotated by 0, 22, 45, 77, and 90° and the second ring was rotated by 0, 22, 45, 77, and 90° for each rotational position of the first ring, resulting in 25 starting structures for each class of co-conformations. It is important to note that in large complicated flexible systems, the global minimum is not especially meaningful. Therefore, our technique is based on developing a representative ensemble of co-conformations so that we have a reliable representation of the density of conformational states function. The theoretical foundations of the methodology are laid out in refs 13 and 14.

The crown ether ring used in these structures is very floppy, as is typical of crown ethers.[15] Though it has no mirror-plane of symmetry, it also lacks an atomic chiral center. Interconversion between different crown configurations, even those of qualitatively different chirality, is therefore facile. Prior research[5] has shown that starting with a single ring conformation structural relaxation can (and does) produce a wide range of final structures

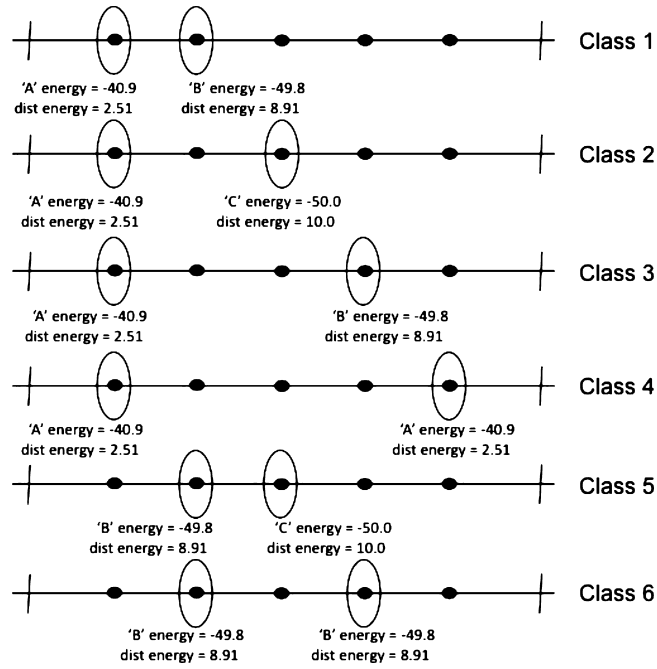

Figure 4. Diagram representing the six classes of coconformations for the five-site [3]rotaxane, annotated with average energies from the [3]rotaxane analysis. Note that the binding energy increases as the ring moves toward the center, but the distortion energy increases as well.

with qualitatively different chirality and yields enantiomers with near equal probability. This result makes it unnecessary to thread the ring in both directions when sampling.

For generation of a set of starting structures, first a graphical-user-interface molecular editor[16] was used to create a basic structure for each class of coconformations. The set of 25 starting structures was then generated for each of the six configuration classes by rotation of the rings about the shaft in the increments noted above.

Because ab initio methods are generally computationally intractable for systems of the size of this rotaxane complex, we have selected semiempirical electronic structure methodology for structural optimizations and single-point energies. It is possible that there may be some empirical force field that would provide results of comparable accuracy at reduced computational expense, but such a force field would almost certainly require atomic charge information since we are treating a charged species. Presumably one would still have to carry out true electronic structure calculations to acquire such atomic charge information, thereby negating much of the benefit of using an empirical potential approach. To select the specific semiempirical method, we note that the intercomponent interactions at work in the rotaxane complexes considered here are dominated by hydrogen bonding. Past research[17] has shown that the AM1 Hamiltonian is reliable for predicting structures and energetic *trends* in complexes governed by hydrogen bonding, so we can be confident in predictions of relative binding-site preference. Additionally, AM1 has been used successfully in the study of rotaxanes that employ the same interaction chemistry as the system considered here, and its limitations are well understood.[5,18] Therefore, all of the structures were fully optimized with the semiempirical AM1 method.[19] Structural optimization of a complex of the size of those treated here is computationally expensive, even when semiempirical electronic structure methodology is employed. For computational efficiency, a script was written to run the 25 calculations for each class of co-conformations serially but distribute the classes across six nodes

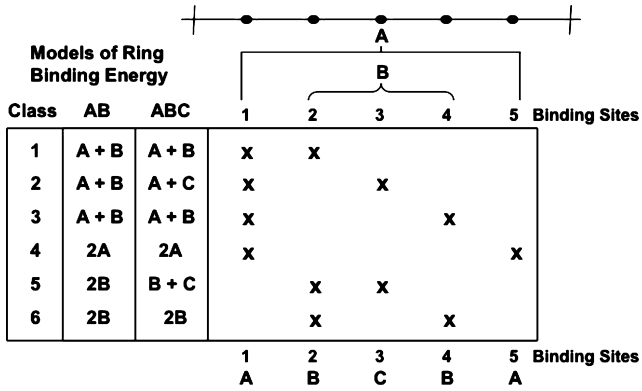

Figure 5. Two models, AB and ABC, were used in our analysis of the binding site preference of the five-sited [3]rotaxane. Model AB assumes all interior sites are the same. The ABC model assumes that the center C site is unique, where B applies only to the two penultimate sites and A the end sites. The chart on the right side of the figure shows the ring binding locations for each of the six classes of co-conformations. The columns at the left specify the expression for the total ring-binding energy for each class of co-conformations and for each of the two models.

of a cluster. Several DFT single-point calculations were also performed to help calibrate the accuracy of the AM1 calculations. All electronic structure calculations were carried out with the GAMESS suite of codes.[20]

Two approaches were taken to analyze the strength of ring binding at each site along the shaft. In the initial analysis, each of the 125 structures was separated into five distinct components: ring1, ring2, [2]rotaxane1 (ring1 removed), [2]rotaxane2 (ring2 removed), and the shaft. (The [2]rotaxane structures are simply the [3]rotaxane structure with either ring1 or ring2 removed.) Ring1 and ring2 are arbitrary names given to distinguish between the rings in order to repeat the calculation the same way for each structure. The rings are chemically identical but may assume different conformations when incorporated into the [3]rotaxane. Single-point calculations were carried out to find the energies of each of the five components while retaining the geometry they had in the optimized [3]rotaxane complex. In addition, full structural optimizations were carried out for the shaft without rings and the ring itself in order to analyze the distortion they undergo when forming a [3]rotaxane structure. Once the energies were found for all 625 structures, Boltzmann statistics were applied to find the Boltzmann-weighted average energy for each of the five parts. (There are 30 contributions to the weighted-average in each case.) The data were then fit to models to analyze the behavior of the rings and shaft upon complexation.

Model

Prior research has shown[5,10] that on a three-site [3]rotaxane that is analogous to the five-site [3]rotaxane being considered here, ring binding at the center site is preferred over the end sites. In the present case of a five-site [3]rotaxane there are three sites that are not "end sites". Consequently, two models of ring binding seem natural. (See Figure 5.) The "AB" model treats ring binding at all interior sites the same way, with no preference among any nonend sites. The "ABC" model treats the center site, "C", as unique from its adjacent penultimate sites, "B". Preliminary calculations were used to establish which of these models is more appropriate to describe the energetics of ring-shaft binding.

Preliminary Analysis. In the ABC model we assume that the total energy of a five-site [3]rotaxane may be approximated by

$$E_{\mathrm{ABC}} \approx \mathrm{f(A,B,C)} = S + 2R + n_{\mathrm{a}}A + n_{\mathrm{b}}B + n_{\mathrm{c}}C \tag{1}$$

where n_{a} is the number of rings on sites of type "A" (end sites), n_{b} is the number of rings on sites of type "B" (penultimate sites), n_{c} is the number of rings on sites of type "C" (central site), S is the total energy of the isolated optimized shaft, and R is the total energy of an isolated optimized ring.

Since there are six classes of co-conformations, there are six computed values of E (each a Boltzmann average of a set of 30 optimized structures). We denote these E_1, E_2, ..., E_6.

The objective is to find the values of A, B, and C that minimize the error function (ε)

$$\varepsilon = \sum_{k=1.66} \{E_k - (S + 2R + n_{ak}A + n_{\mathrm{b}k}B + n_{ck}C)\}^2 \tag{2}$$

For class $k = 1$, $n_{\mathrm{a}} = 1$, $n_{\mathrm{b}} = 1$, $n_{\mathrm{c}} = 0$. For class $k = 2$, $n_{\mathrm{a}} = 1$, $n_{\mathrm{b}} = 0$, $n_{\mathrm{c}} = 1$. For class $k = 3$, $n_{\mathrm{a}} = 1$, $n_{\mathrm{b}} = 1$, $n_{\mathrm{c}} = 0$. For class $k = 4$, $n_{\mathrm{a}} = 2$, $n_{\mathrm{b}} = 0$, $n_{\mathrm{c}} = 0$. For class $k = 5$, $n_{\mathrm{a}} = 0$, $n_{\mathrm{b}} = 1$, $n_{\mathrm{c}} = 1$. For class $k = 6$, $n_{\mathrm{a}} = 0$, $n_{\mathrm{b}} = 2$, $n_{\mathrm{c}} = 0$.

The values of A, B, and C are determined by linear least-squares analysis. Similar analysis was carried out for the AB model, in which it is effectively assumed that $B = C$ (i.e., in which all nonend-sites have identical ring binding). On the basis of this assumption, the model may be written

$$E_{\mathrm{AB}} \approx \mathrm{f(A,B)} = S + 2R + n_{\mathrm{a}}A + n_{\mathrm{b}}B \tag{3}$$

The values computed for each model using this preliminary analysis are given in Table 1. We note that the residual error is significantly lower in the case of the ABC model as shown in Table 1. These preliminary studies reveal that the "C" site is unique from the penultimate "B" sites.

[3]Rotaxane Analysis. On the basis of the above preliminary results, we selected the ABC model for further analysis. To do so, for any selected [3]rotaxane configuration, we identified eight total energies that may be computed directly with electronic structure calculations: E(ring1), SP energy of ring1; $E(\mathrm{ring}^{\mathrm{opt}}) = E(\mathrm{ring1}^{\mathrm{opt}}) = E(\mathrm{ring2}^{\mathrm{opt}})$, energy of optimized ring; E(ring2), SP energy of ring2; E([3]rotaxane); E([2]rotaxane1), energy of rotaxane with ring 2 missing; E([2]rotaxane2), energy of rotaxane with ring 1 missing; E(shaft), SP energy of shaft; $E(\mathrm{shaft}^{\mathrm{opt}})$, energy of optimized shaft.

TABLE 1: Total Binding Energies from the Preliminary, [2]Rotaxane, AM1 Single Point, and DFT Single Point Analyses in kcal/mol

A	*B*	*C*	rms error
	AB Model		
−38.2	−39.5		2.3
	ABC Model		
−37.7	−40.8	−38.9	0.29
	[2]Rotaxane Analysis		
−38.7	−40.3	−38.4	
	AM1 SP analysis		
−51.4	−52.5	−49.2	
	DFT SP Analysis		
−60.9	−63.8	−56.0	

From these eight total energies we seek to find: BE1 = binding energy of ring 1; Edr1 = distortion energy of ring 1 upon forming the rotaxane; BE2 = binding energy of ring 2; Edr2 = distortion energy of ring 2 upon forming the rotaxane; Err = ring−ring interaction energy; Eds = distortion energy of shaft upon forming the rotaxane. When the [3]rotaxane is optimized, a ring placed at binding site A does not assume the same configuration as a ring placed at binding site B (or C). E(ring1) is the (single point) energy of isolated ring1, in the structure it assumes upon full optimization of the rotaxane. Similarly, E(ring2) is the energy of isolated ring2, in the structure it assumes upon full optimization of the rotaxane. When these rings are isolated and fully optimized, they assume the same structure, since they are chemically identical, so E(ring1opt) = E(ring2opt). For example, the energy difference E(ring1) − E(ring1opt) = Edr1, the distortion energy of ring1.

We can compute these values by considering the following "reactions"

$$\text{ring1} + \text{[2]rotaxane2} \rightarrow \text{[3]rotaxane} \quad (4.1)$$

$$\Delta E_1 = \text{BE1} + \text{Err}$$

$$\text{ring1}^{\text{opt}} + \text{[2]rotaxane2} \rightarrow \text{[3]rotaxane} \quad (4.2)$$

$$\Delta E_2 = \text{BE1} + \text{Edr1} + \text{Err}$$

$$\text{ring2} + \text{[2]rotaxane1} \rightarrow \text{[3]rotaxane} \quad (4.3)$$

$$\Delta E_3 = \text{BE2} + \text{Err}$$

$$\text{ring2}^{\text{opt}} + \text{[2]rotaxane1} \rightarrow \text{[3]rotaxane} \quad (4.4)$$

$$\Delta E_4 = \text{BE2} + \text{Edr2} + \text{Err}$$

$$\text{ring1} + \text{ring2} + \text{shaft} \rightarrow \text{[3]rotaxane} \quad (4.5)$$

$$\Delta E_5 = \text{BE1} + \text{BE2} + \text{Err}$$

$$\text{ring1}^{\text{opt}} + \text{ring2}^{\text{opt}} + \text{shaft}^{\text{opt}} \rightarrow \text{[3]rotaxane} \quad (4.6)$$

$$\Delta E_6 = \text{BE1} + \text{Edr1} + \text{BE2} + \text{Edr2} + \text{Err} + \text{Eds}$$

ΔE_i for $i = 1, ..., 6$, can be computed from the calculated energies of the structures.

$$\Delta E_1 = E(\text{[3]rotaxane}) - E(\text{[2]rotaxane2}) - E(\text{ring1}) \quad (5.1)$$

$$\Delta E_2 = E(\text{[3]rotaxane}) - E(\text{[2]rotaxane2}) - E(\text{ring1}^{\text{opt}}) \quad (5.2)$$

$$\Delta E_3 = E(\text{[3]rotaxane}) - E(\text{[2]rotaxane1}) - E(\text{ring2}) \quad (5.3)$$

$$\Delta E_4 = E(\text{[3]rotaxane}) - E(\text{[2]rotaxane1}) - E(\text{ring2}^{\text{opt}}) \quad (5.4)$$

$$\Delta E_5 = E(\text{[3]rotaxane}) - E(\text{ring1}) - E(\text{ring2}) - E(\text{shaft}) \quad (5.5)$$

$$\Delta E_6 = E(\text{[3]rotaxane}) - E(\text{ring1}^{\text{opt}}) - E(\text{ring2}^{\text{opt}}) - E(\text{shaft}^{\text{opt}}) \quad (5.6)$$

This analysis yields six equations (4.1−4.6) that we can solve simultaneously for the six unknowns, (BE1, Edr1, BE2, Edr2, Err, Eds). When these unknowns are found for each class of coconformations, the analysis produces multiple estimates for some of the values. Consulting Figure 5, it can be seen that the binding energy for a ring at site "A", is found five times, resulting in five estimates of "A". Similarly, five estimates of "B" and two estimates of "C" were found. These sets were averaged to find the final values of sites A, B, and C. The associated distortion energies were found similarly.

[2]Rotaxane Analysis. Note that several of the values can also be estimated from a subset of the eight computed total energies. Consider the following five "reactions" to form a [2]rotaxane

$$\text{ring1} + \text{shaft} \rightarrow \text{[2]rotaxane1} \quad (6.1)$$

$$\Delta E_7 = \text{BE1}$$

$$\text{ring1}^{\text{opt}} + \text{shaft} \rightarrow \text{[2]rotaxane1} \quad (6.2)$$

$$\Delta E_8 = \text{BE1} + \text{Edr1}$$

$$\text{ring2} + \text{shaft} \rightarrow \text{[2]rotaxane2} \quad (6.3)$$

$$\Delta E_9 = \text{BE2}$$

$$\text{ring2}^{\text{opt}} + \text{shaft} \rightarrow \text{[2]rotaxane2} \quad (6.4)$$

$$\Delta E_{10} = \text{BE2} + \text{Edr2}$$

$$\text{ring2}^{\text{opt}} + \text{shaft}^{\text{opt}} \rightarrow \text{[2]rotaxane2} \quad (6.5)$$

$$\Delta E_{11} = \text{BE2} + \text{Edr2} + \text{Eds}$$

ΔE_i for $i = 7, ..., 11$, can be computed from the energies from electronic structure calculations.

$$\Delta E_7 = E(\text{[2]rotaxane1}) - E(\text{shaft}) - E(\text{ring1}) \quad (7.1)$$

$$\Delta E_8 = E([2]\text{rotaxane1}) - E(\text{shaft}) - E(\text{ring1}^{\text{opt}}) \quad (7.2)$$

$$\Delta E_9 = E([2]\text{rotaxane2}) - E(\text{shaft}) - E(\text{ring2}) \quad (7.3)$$

$$\Delta E_{10} = E([2]\text{rotaxane2}) - E(\text{shaft}) - E(\text{ring2}^{\text{opt}}) \quad (7.4)$$

$$\Delta E_{11} = E([2]\text{rotaxane2}) - E(\text{ring2}^{\text{opt}}) - E(\text{shaft}^{\text{opt}}) \quad (7.5)$$

This gives five equations (6.1−6.5) that are solved simultaneously for the five unknowns, (BE1, Edr1, BE2, Edr2, Eds). The values of total binding are then computed and compared to those from the preliminary analysis in Table 1. The agreement is very good. Because the results of this [2]rotaxane analysis (eqs 6.1−7.5) are based on a subset of energies, they are likely less reliable than those from the full [3]rotaxane analysis (eqs 4.1−5.6), but the close agreement among the three approaches serves as a valuable cross check. As an additional measure of the accuracy of the semiempirical calculations, crude estimates of the *A*, *B*, and *C* binding energies, based only on eqs 5.1 and 5.3, were calculated at both the AM1 and DFT/B3LYP/6-31G levels of theory. The results, included in Table 1, show that AM1 likely underestimates the binding energies but recovers the same trends as DFT.

Results and Discussion

Preliminary analysis using the AB model produced a result consistent with previously published results for an analogous three-site [3]rotaxane,[5,10] that the interior binding sites have lower energy than the terminal binding sites. More detailed analysis with the ABC model, however, reveals that it is inaccurate to describe all interior sites as the same. (See Table 1.) The difference in energy between the different interior sites, B and C, was found to be greater than the difference between the end site and the center site, A and C.

Before embarking on the present analysis it was our first hypothesis that site A would be least preferred, then B, and then C based on the reasoning that ring binding at site C produces the most possible intercomponent atom−atom interactions. The calculations reveal that site B has the lowest binding energy. Why? The reason is revealed by the detailed partitioning of the interaction energy.

As shown in Table 2, the strength of ring binding actually increases as the binding site moves toward the center of the shaft,[5] consistent with the reasoning in the above paragraph, This energy, however, only measures the strength of the ring−shaft binding. In order for ring binding to take place, the shaft and ring must undergo distortion to assemble the rotaxane. Referring to Table 2, the distortion energy required for binding

TABLE 2: Energies Found from [3]Rotaxane Analysis in kcal/mol[a,a]

	A	B	C
binding energy	−40.9	−49.8	−50.0
ring distortion	2.51	8.91	10.0
total binding	−38.3	−40.9	−40.0

[a] Shaft distortion energy is 0.63 kcal/mol; ring/ring interaction energy is 1.26 kcal/mol.

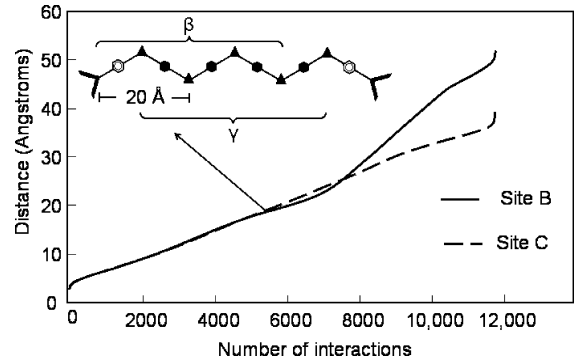

Figure 6. Atom−atom distances for all pairwise interactions between the crown ether ring on a particular binding site and the shaft, after optimization. The interactions are ordered by distance, and distance is plotted versus interaction number. Notice that above 25 Å there are over 4000 interactions where site C is more tightly constricted compared to site B. Sites B and C are essentially identical up to 20 Å, as seen by comparing areas β and γ. Between 20 and 25 Å, site B has a cluster of interactions around the same length due to the shaft-terminating stopper. Above 25 Å the B site has interactions only on one side, leaving it less constricted than site C.

Figure 7. Initial shaft structure (ball-and-cylinder rendering) and six final shaft structures (wires rendering) that are produced upon full optimization of the six different classes of coconformations of the [3]rotaxane. Note the limited range of distortion of the shaft.

at site B is notably lower than that required for binding at site C. Insight into why the ring distortion cost of binding at site C exceeds that for binding at site B is afforded by Figure 6. The figure shows the intercomponent atom−atom distances ordered from closest to farthest for the cases of ring binding at site B and ring binding at site C. It is clear that the local geometries are essentially identical, but beyond 25 Å site C is much more constrained than site B. Since there are over 4000 interactions in this more constrained region, their aggregate effect produces the site's higher distortion cost. The total energy gain is −40.9 and −40.0 kcal/mol for binding at the B and C sites, respectively, making binding at site B energetically favored, due to the influence of long-range intercomponent interactions. Because semiempirical electronic structure methods are employed here, there is no expectation of high accuracy for the absolute quantitative magnitudes of the energies reported, but the ability of AM1 to correctly order hydrogen bond strengths[21] allows us to extract the *relative* importance of these different intercomponent hydrogen-bonding interactions in the [3]rotaxane complex. The preliminary analysis also found the order of site preference; B, C, then A, but the decomposition analysis reveals the *why* behind the [3]rotaxane site preference and also provides information that is directly comparable to previous studies.

Previous studies of the analogous three-sited [3]rotaxane,[5] revealed shaft distortion energy and ring−ring interaction energy to be negligible. Our analysis reports equivalent results for the five-site [3]rotaxane. The low average-shaft-distortion energy (0.73 kcal/mol) is approximately three times weaker than that of site A's ring distortion energy, which is the weakest among the three binding sites. Also, the ring−ring interaction, (0.11 kcal/mol) is an order-of-magnitude less than the shaft distortion energy. This is to be expected for the ring−ring interaction energy, since the principal difference between the two systems is a longer shaft in the present case, giving the rings more opportunity to be farther apart, therefore lowering the average

ring−ring interaction energy. The limited degree of distortion of the shaft is shown in Figure 7, which uses ball-and-cylinder rendering to depict the initial shaft structure and wire rendering to show six final shaft structures produced upon full optimization of structures from the six classes of coconformations of the [3]rotaxane.

Conclusions

Ring-binding site preference in a five-site [3]rotaxane follows some of the same general trends found in a previous study of a three-site [3]rotaxane.[5] For site preference, ring binding at interior sites is preferred over binding at end sites. There is very little ring−ring interaction, and as with the three-site [3]rotaxane, there is negligible shaft distortion.

In order to accurately describe the site preference of the rings along the five-sited shaft, a model that differentiates between interior sites must be used (ABC model). Overall, ring binding at B sites (penultimate sites) is energetically preferred. This preference arises from a competition between two factors: the site's ring-binding energy and the energy cost to distort the ring to place it on that site. As the ring moves toward the center of the shaft, its binding energy increases; however, it also costs more energy to distort the ring to accomplish binding at sites farther from the end of the shaft due to the aggregate effect of many long-range interactions. These two competing factors combine to determine binding site preference. This is very different from a conventional macroscopic abacus where the energy is essentially independent of the position of a bead or the relative orientation of adjacent beads. Synthesis of an unbiased molecular abacus will need to address this challenge. The analysis by which these competing factors can be extracted from electronic structure calculations may be generalized to more complex rotaxanes and should prove to be a valuable tool for their analysis.

Acknowledgment. The authors thank Dr. Xiange Zheng for the crown ether ring starting structure. Financial support was provided by the Drexel STAR scholars program (J.P.A.) and NSF CHE0449595.

Supporting Information Available: Listings of atomic coordinates of all optimized rotaxanes. This material is available free of charge via the Internet at http://pubs.acs.org.

References and Notes

(1) Kay, E. R.; Leigh, D. A.; Zerbetto, F. *Angew. Chem., Int. Ed.* **2007**, 72.
(2) Frankfort, L.; Zheng, X.; Sohlberg, K. *Encycl. Nanosci. Nanotechnol.* **2004**, *5*, 73.
(3) Raymo, F. M.; Bartberger, M. D.; Houk, K. N.; Stoddart, J. F. *J. Am. Chem. Soc.* **2001**, *123*, 9264.
(4) Raymo, F. M.; Houk, K. N.; Stoddart, J. F. *J. Org. Chem.* **1998**, *63*, 6523.
(5) Zheng, X.; Sohlberg, K. *J. Phys. Chem. A* **2006**, *110*, 11862.
(6) Foster, M. E.; Sohlberg, K. *J. Chem. Theory Comput.* **2007**, *3*, 2221.
(7) Nakazono, K.; Oku, T.; Takata, T. *Tetrahedron* **2007**, *48*, 3409.
(8) Sato, T.; Takata, T. *Tetrahedron* **2007**, *48*, 2797.
(9) Leigh, D. A.; Thompson, A. R. *Tetrahedron* **2008**, *64*, 8411.
(10) Chiu, S. H.; Rowan, S. L.; Cantrill, S. J.; Stoddart, J. F.; White, A. J. P.; Williams, D. L. *Chem.−Eur. J.* **2002**, 5170.
(11) Chiu, S. H.; Elizarov, A. M.; Glink, P. T. *Org. Lett.* **2002**, *4*, 3561.
(12) Frankfort, L.; Sohlberg, K. *Materials Research Society Symposium Proceedings: Nano- and Microelectricalmechanical Systems (NEMS and MEMS) and Molecular Machines* **2003**, *741*, J7.4.1.
(13) Zheng, X.; Sohlberg, K. *J. Phys. Chem.* **2003**, *107*, 1207.
(14) Zheng, X.; Sohlberg, K. *Phys. Chem. Chem. Phys.* **2004**, *6*, 809.
(15) An, H.; Bradshaw, J. S.; Izatt, R. M. *Chem. Rev.* **1992**, *92*, 543.
(16) *Hyperchem. 6.02 ed.*; Hypercube Inc.: Waterloo, Ontario, Canada, 2000.
(17) Fabian, W. M. F. *J. Comput. Chem.* **1988**, *9*, 369.
(18) Frankfort, L.; Sohlberg, K. *THEOCHEM* **2003**, *621*, 253.
(19) Dewar, M. J. S.; Zoebisch, E. G.; Healy, E. F.; Stewart, J. J. P. *J. Am. Chem. Soc.* **1985**, *107*, 3902.
(20) Schmidt, M. W.; Baldridge, K. K.; Boatz, J. A.; Elbert, S. T.; Gordon, M. S.; Jensen, J. H.; Koseki, S.; Matsunaga, N.; Nguyen, K. A.; Su, S.; Windus, T. L.; Dupuis, M.; Montgomery, J. A. *J. Comput. Chem.* **1993**, *14*, 1347.
(21) Buemi, G.; Zuccarello, F.; Raudino, A. *THEOCHEM* **1988**, *164*, 379.

JP8106099